JOM, Vol. 64, No. 10, 2012
DOI: 10.1007/s11837-012-0439-5
© 2012 TMS

Embedded Binary Eutectic Alloy Nanostructures

D. C. CHRZAN,[1,2,7] S. J. SHIN,[3] J. GUZMAN,[1,2] C.-W. YUAN,[1,2] C. Y. LIAO,[1,2] P. R. STONE,[1,2] C. N. BOSWELL-KOLLER,[1,2] C. A. SAWYER,[1,2] K. C. BUSTILLO,[1,2] M. P. SHERBURNE,[1] T. CONRY,[1,2] R. R. LIETEN,[4] O. D. DUBON,[1,2] A. M. MINOR,[1,5] M. WATANABE,[6] J. W. BEEMAN,[2] K. M. YU,[2] J. W. AGER III,[2] and E. E. HALLER[1,2]

1.—Department of Materials Science and Engineering, University of California, Berkeley, CA 94720, USA. 2.—Materials Sciences Division, Lawrence Berkeley National Laboratory, Berkeley, CA 94720, USA. 3.—Lawrence Livermore National Laboratory, Livermore, CA 94551, USA. 4.—Department of Physics and Astronomy, K. U. Leuven, 3001 Leuven, Belgium. 5.—National Center for Electron Microscopy, Lawrence Berkeley National Laboratory, Berkeley, CA 94720, USA. 6.—Department of Materials Science and Engineering, Lehigh University, Bethlehem, PA 18015, USA. 7.—e-mail: dcchrzan@berkeley.edu

The properties of binary eutectic alloy nanostructures embedded within a matrix are discussed. It is demonstrated that GeAu and GeSn nanostructures embedded in SiO_2 form in a bilobed structure as predicted by a simple theory. Upon heating, the nanostructures melt and assume a nominally compositionally homogeneous structure. Slow cooling of the liquid returns the nanostructure to its equilibrium bilobed morphology. Rapid quenching yields a kinetically limited, nearly compositionally homogeneous solid. Rapid thermal annealing can convert this metastable structure again into the bilobed structure. It is, therefore, possible to switch between the bilobed structure and the homogenous structure. The kinetics of the homogeneous composition to bilobe structure transformation depend on composition. Tuning the composition enables one to tune the transformation temperature. Possible technological applications of these nanostructures are discussed.

INTRODUCTION: EMBEDDED NANOSTRUCTURES

The promise of controlling matter at the nanoscale is manifest. One expects that nanoscaled materials will display both interesting electronic and optical behaviors, as well as interesting structural properties. Consequently, there has been great effort devoted to fabricating and characterizing nanostructures of various morphologies.

A common morphology is a simple nanocrystal. Nanocrystals are often synthesized using solution chemistry wherein one takes advantage of the control offered by such methods to produce nanocrystals within an organic solvent. This approach is remarkably powerful. It can produce a wide variety of nanostructures with nearly monodisperse size distributions.[1] However, the nanostructures as produced are best viewed as free standing, and incorporation within a device requires that the structures be manipulated into the configuration desired for a given application. Furthermore, the list of materials that can be fabricated is limited by the chemical properties of the constituents.

An alternative approach is to fabricate the nanostructures within a matrix. One common approach is ion beam synthesis (IBS). During IBS of nanocrystals, ions are accelerated and implanted within a matrix. Typically, the implanted ions are chosen so that their solubility within the matrix is minimal. During the implantation process, the solubility limit of the ions is reached, and nanostructures begin to form within the matrix through what is essentially a precipitation process. Typically, ion implantation is followed by thermal annealing, and the net result is an array of nanostructures embedded within the starting matrix.[2]

IBS is complementary to chemical synthesis methods. For example, the implantation process is not limited by the same chemistry governing chemical synthesis. As a result, synthesis of Si and Ge

 (Published online August 31, 2012)

nanocrystals, materials that present a challenge for chemical synthesis approaches, is straightforward. Furthermore, IBS nanostructures can be positioned in desired locations during fabrication. This avoids the need to arrange nanoscale objects into desired configurations after the objects have been synthesized. Moreover, the nanostructures are embedded within a matrix. Typically, the properties of a nanostructure are governed by nanostructure-matrix interaction: Different choices for the matrix material necessarily lead to different physical properties. Thus, the matrix provides an additional degree of freedom that can be exploited to produce materials with remarkable properties. Finally, IBS, based on mass spectrometry, is an inherently clean process.

However, IBS has a few serious limitations. For example, the size distributions of nanocrystals typically obtained through IBS are much broader than those that can be achieved using direct chemical synthesis. In one sense, the point of nanostructures is that their physical properties are size dependent. Samples with a broad range of sizes tend to produce a response to stimulation that somehow represents the size distribution of nanocrystals rather than the response of an individual nanocrystal. In the case where a collective response from the distribution of nanocrystals is sought, a broad range of nanocrystal sizes might prevent collective electronic and optical responses that could be observed otherwise. Another drawback to IBS is that one can only synthesize limited volumes of material. This can frustrate characterization efforts, as well as efforts to exploit the properties of the nanostructures.

Despite these shortcomings, however, the resulting nanostructures are still of substantial interest. As an example, this article considers the fabrication and characterization of the properties of binary eutectic alloy nanocrystals (BEANs) embedded in silica. More specifically, we consider experimentally the phase transformation kinetics of these structures and show that they may solidify into (at least) two states, and we argue that these two states have different physical properties. We demonstrate that the structures can be cycled between the two states repeatedly, and we suggest that this cycling may serve technological ends.

BILOBED, BICRYSTALLINE NANOSTRUCTURES

Solidification of eutectic alloys is a known and established route to tailoring the structure of alloys at the nanoscale. In common circumstances, the volume of the alloy is macroscopic, and processing is aimed at introducing a desired structure at the nanoscale, largely through control of the precipitation process. Of course, the phase diagram serves as a guide to the development of these desired processing routes. Naturally, great effort has been directed toward computing phase diagrams of alloys, and the advances enabled are substantial.

What remains as a challenge, however, is the control of the structure within nanoscale volumes of eutectic alloys. The starting point for developing this control is an understanding of the equilibrium nanostructures that one might observe. The stable nanostructures are determined by both volumetric and surface/interfacial contributions to the free energy. Because the surface/interfacial contribution can vary substantially with orientation, the phase space of allowed structures becomes quite complicated.

The problem is simplified substantially if one assumes that the interfacial free energies influencing structural stability are isotropic. This assumption is reasonable for a liquid droplet embedded within an amorphous material, or for one amorphous material embedded within another. In other circumstances, the model can serve as an approximate guide to the structures that might be observed in more complicated situations.

In Yuan et al.,[3] a model for the structural stability of BEANs was introduced. The relative stability of competing structures is governed by isotropic interfacial free energies. Furthermore, the model assumes that the matrix material is fully relaxed. With these assumptions, the equilibrium stable nanostructure is a function of two dimensionless interfacial free energies only: $\gamma_1 \equiv \gamma_{\alpha/M} \big/ \gamma_{\alpha/\beta}$ and $\gamma_2 \equiv \gamma_{\alpha/M} \big/ \gamma_{\alpha/\beta}$, where $\gamma_{i/j}$ is the interfacial free energy between phases i and j, and M represents the matrix. As shown in Fig. 1, for an α/β phase alloy, three equilibrium nanostructure morphologies are possible: (I) completely separated α and β nanocrystals, (II) core/shell nanocrystals (both α-shell/β-core and β-shell/α-core,

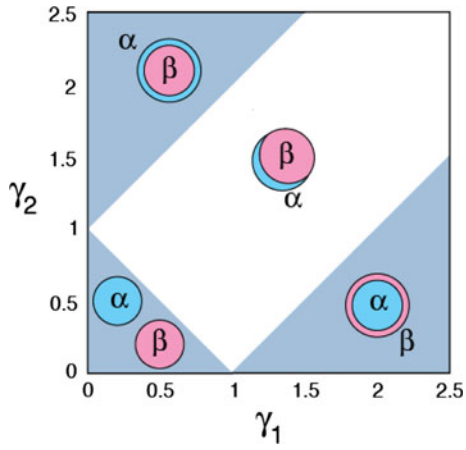

Fig. 1. Equilibrium structures expected for BEANs based on the assumption of isotropic interfacial free energies (following Ref. 3). The dimensionless interfacial free energies are defined as $\gamma_1 \equiv \gamma_{\alpha/M} \big/ \gamma_{\alpha/\beta}$ and $\gamma_2 \equiv \gamma_{\alpha/M} \big/ \gamma_{\alpha/\beta}$, where $\gamma_{i/j}$ is the interfacial free energy between phases I and j, and M represents the matrix. The shaded regions depict differing regions of structural stability, and a typical structure within each region is shown. For example, the white region in the central portion of the stability map represents the combination of interfacial free energies for which one expects a bilobed nanostructure to be stable. GeSn and GeAu embedded in SiO_2 both form bilobed structures (Color figure online).

and (III) bilobed nanocrystals (one lobe α and the other β). Moreover, this model predicts that if the dimensionless values of the interfacial free energies do not depend on composition, then the morphology (e.g., bilobed versus core/shell) of the resulting nanostructures is independent of the volume fraction of the α and β phases.

IBS offers a convenient way to explore the stability of embedded nanostructures experimentally. For example, GeSn nanocrystals have been fabricated by first implanting Sn, subsequently implanting Ge, and then annealing.[4] Bilobed nanocrystals are formed, as shown in Fig. 2a. The nanocrystals nucleate and grow during implantation. However, at this stage, the nanostructures are most likely amorphous due to the damage induced by the ion beam. The post implantation annealing both crystallizes and coarsens the nanocrystals.

We have also fabricated GeAu bilobed nanocrystals using a combination of sputtering and IBS (Fig. 2d).[5] More specifically, Ge ions are implanted within a cosputtered layer composed of Au and SiO_2. Postimplantation annealing results in an array of GeAu nanocrystals also embedded within SiO_2. In both of these cases, the morphologies are very similar, suggesting that the free energies of the Ge/SiO_2 interface and the Metal/SiO_2 interface are not too different (both fall within the white region shown in Fig. 1).

PROPERTIES: CONTROL OF PHASE TRANSFORMATIONS

Once formed, the embedded BEANs provide a system in which to study the thermodynamics of phase transformations for these embedded nanostructures. If one neglects the effects of coarsening (a reasonable approximation for many of the experiments considered here), then one can think of each BEAN as being enclosed within its own test tube. This enables temperature cycling of the system, enabling the observation of *both* melting and solidification within the same set of particles. (Typically, it is not possible to do this with free-standing nanocrystals where one is often limited to exploration of the melting behavior only.) Furthermore, the melting and solidification rates can be varied, and the effects of these variations were studied.

The starting point for understanding what might happen during these experiments is the bulk phase diagram. Figure 3 presents the bulk phase diagram for the GeSn system. GeSn forms a eutectic, with the eutectic composition very near to pure Sn. After implantation, the sample is heated to 900°C. For sufficiently Sn-rich BEANs, the bulk phase diagram predicts that the BEANs will melt completely, resulting in nominally compositionally homogeneous liquid BEANs.

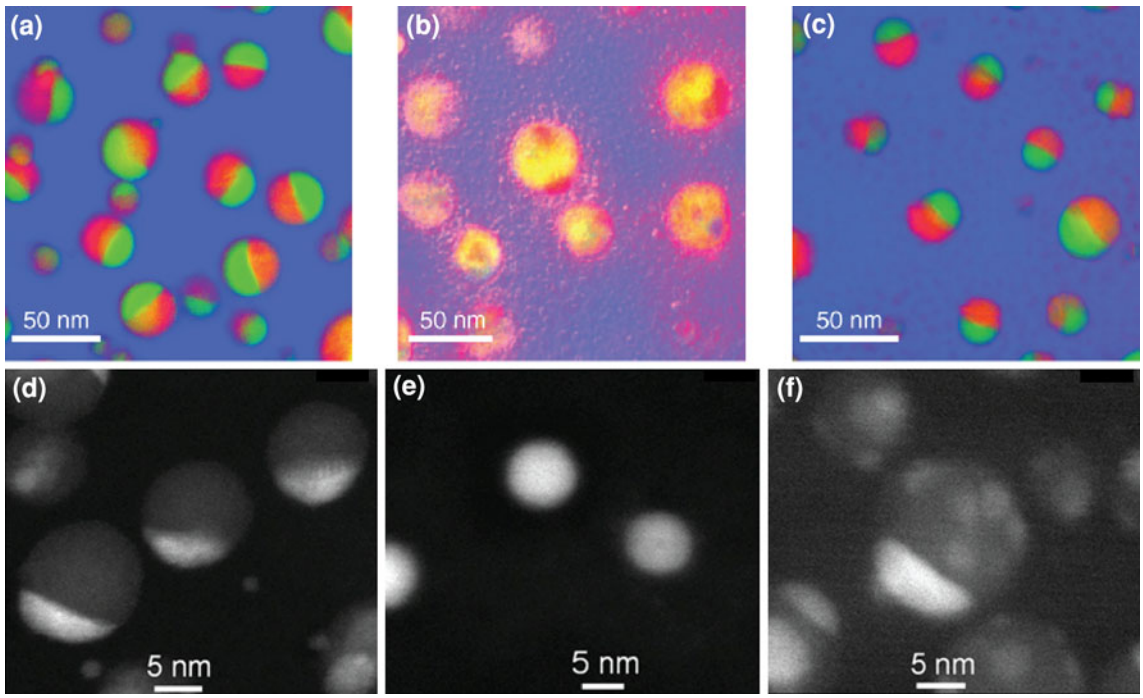

Fig. 2. (a–c) Energy-filtered transmission-electron microscopy images of (a) as grown, (b) post-PLM, and (c) post-RTA at 400°C for 10 s (from Ref. 4). Here, red represents Ge, green Sn, and blue SiO_2. Yellow regions represent a mixture of Ge and Sn atoms. (d–f) HAADF-STEM images of GeAu nanostructures (d) as grown, (e) post-PLM, and (f) post-RTA at 300°C for 10 s (from Ref. 5). The bright regions correspond to Au-rich compositions. Note the change in scale between the GeSn and GeAu nanostructures. In both cases, PLM leads to homogenization of the composition. For GeSn, nanostructures appear to fragment during the process. RTA restores the bilobed structures (Color figure online).

Consider two limiting cooling rates: infinitely slow cooling, and rapid quenching. For the infinitely slow cooling case, one expects the cooling sequence to proceed as shown in Fig. 3. The entire sample will remain liquid until the temperature of the liquid reaches the liquidus line. Here, a solid phase consisting primarily of Ge will begin to precipitate. The preferential precipitation of Ge atoms will cause the liquid composition to shift in the pure Sn direction, and its melting point will be reduced. A further reduction in temperature will lead to more Ge precipitation into the solid phase, and further Sn enrichment of the liquid. As the temperature is lowered, the liquid composition will continue to track the liquidus, and the solid will continue to precipitate coming to equilibrium at all temperatures, thus changing composition slightly according to the phase diagram. When the eutectic temperature is reached, the solidification will be complete. Since at each temperature the structure reaches equilibrium, there will be only one solid nucleus, as this minimizes the interfacial free energy. The final result will be a bilobed nanostructure, one lobe consisting of nearly pure Ge, the other of nearly pure Sn. This is the structure predicted from the simple analysis and also observed experimentally.

At the other extreme, consider rapidly quenching from the liquid state. In the extreme case, this quench proceeds so rapidly that the segregation of atoms to their equilibrium structure is not possible. Instead, one arrives at a metastable state in which the liquid alloy merely passes through the glass transition, yielding amorphous and nearly compositionally homogeneous BEANs, as shown by the purple arrow in Fig. 3.

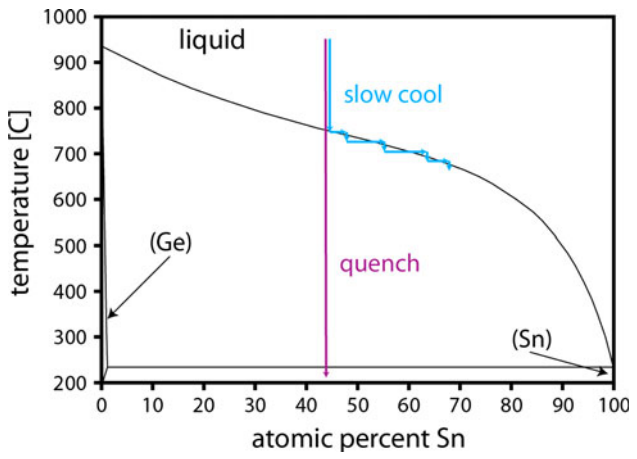

Fig. 3. The phase diagram of the bulk GeSn system (following Ref. 13). Assuming that the nanoscale phase diagram does not differ from the bulk, one can identify two limiting cooling rates. In the limit of a very slow cool, the composition of the liquid will track the liquidus line as shown in blue, continuing until the eutectic temperature is reached. For a rapid quench, the system will not have time to segregate and will assume a kinetically limited, compositionally homogeneous structure, as shown in purple (Color figure online).

It is useful to estimate the quench rate required to prevent the equilibrium structure from forming. This rate can be estimated by considering the diffusion length within the liquid alloy during solidification. As an example, consider the diffusion coefficient for Ge in Au liquid given by Wernick.[6] From this reference, one estimates that the diffusion coefficient depends on temperature according to $D = D_o \exp[-\Delta E/k_B T]$ with $D_o = 1.76$ cm^2/s, $\Delta E = 0.722$ eV, k_B Boltzmann's constant, and T is the temperature in K. Noting that the diffusion length $\bar{l}$ under variable temperature conditions is given by

$$\bar{l} = \sqrt{\int_{t_o}^{t_f} 6D[T(t)]dt}$$

where $T(t)$ is the temperature at time t, and $t_o(t_f)$ is the initial (final) time spanning the times associated with solidification. As a rough estimate, we choose t_o to correspond to that time at which the liquid alloy reaches the solidification temperature of bulk Ge and t_f to correspond to the time at which the liquid reaches the eutectic temperature of bulk AuGe, and assuming that the temperature is reduced linearly in time with a rate θ, one finds that a cooling rate of approximately $\theta \approx 4 \times 10^{11}$ K/s leads to a diffusion length of approximately 20 nm (Fig. 4). Note that quench rates this fast imply that the solidification process occurs in less than a nanosecond. Cooling rates faster than this will inhibit separation of the Ge and Au during solidification of the nanocrystal. Cooling rates slower than this might allow separation during cooling. The quench rates necessary to prevent segregation seem to be extreme. However, quench rates this rapid are accessible under the conditions of pulsed laser melting,[7] and it is interesting to explore experimentally if pulsed laser melting (PLM) can be used to stabilize a compositionally homogeneous structure.

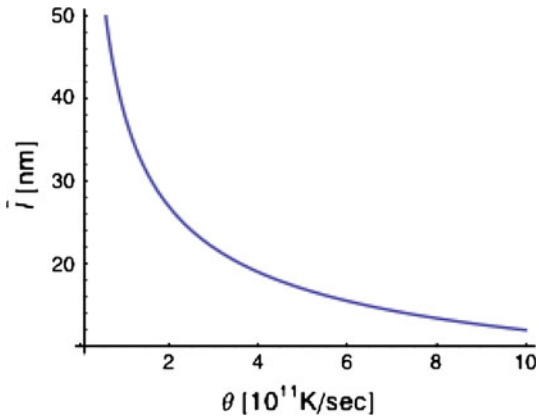

Fig. 4. The diffusion length during quenching estimated for the GeAu eutectic liquid solidification process as a function of cooling rate, θ computed using the model described in the text.

Accordingly, we have used PLM to process both GeAu and GeSn nanostructures. In their initial state, the nanostructures are bilobed, bicrystalline in structure, and embedded within a silica matrix grown on a silicon substrate. The samples are exposed to a single 248 nm pulse of an eximer laser with a fluence of 0.3 J/cm^2. This raises the sample temperature substantially and melts the embedded nanostructures.[8] Immediately after the pulse, the sample begins to cool, and presumably, the nanostructures resolidify. The nanostructures are then examined using transmission electron microscopy (TEM), extended x-ray absorption fine structure, x-ray scattering, and Raman spectroscopy.

Figure 2 shows TEM images of both the GeSn and GeAu nanostructures in their initial state and after PLM. In both circumstances, PLM leads to nanostructures that appear nearly compositionally homogeneous based on microscopy experiments (for GeAu HAADF-STEM, and for GeSn energy filtered TEM). Further analysis of the GeAu case using x-ray diffraction shows that the GeAu nanostructures contain metastable crystalline phases—the hexagonal close-packed β-phase, and crystalline Au and Ge as well. A similar analysis was not carried out for the GeSn nanostructures.

These initial PLM experiments confirm that cooling during PLM is rapid enough to prevent equilibration of the BEANs. Further evidence that this is the case can be gleaned from subsequent rapid thermal annealing (RTA) experiments. Figure 2c shows the GeSn structures after RTA at 400°C for 10 s. Figure 2f shows the GeAu nanostructures after RTA at 300°C for 10 s. Note that in both cases, bilobed structures are restored by RTA. However, there are also slight differences from the initial structures. In the case of GeAu, there seem to be a number of second phase nuclei associated with the Ge portion of some of the bilobed structures.

In the case of GeSn, RTA leads to bilobed structures, but a substantial debris field (from PLM) remains. Theory suggests that this is the behavior expected and is due to the extreme temperatures reached during PLM (3,000 K).[8] Theory predicts that for a pure Ge nanocrystal, the solubility of Ge in the matrix increases substantially during PLM, and Ge atoms desorb from the nanostructures. During the rapid cooling portion of a typical PLM experiment, the desorbed atoms are "frozen" within the matrix, or they nucleate into very small clusters. The subsequent RTA leads to growth of the clusters, which then become visible within TEM experiments. If annealing continues, then theory predicts that the larger nanocrystals will consume these smaller clusters. Interestingly, theory also predicts that under these circumstances, PLM will lead to a narrower distribution of nanocrystal sizes.[8]

For the case of GeAu, the PLM-RTA cycle has been repeated 10 times within a single sample.[5] In the final state, the nanocrystals are essentially bilobed. This implies that the process can be cycled repeatedly.

The ability to cycle between a stable and a metastable structure suggests intriguing possibilities. First and foremost, the electrical properties of the two structures are expected to be markedly different. The compositionally homogeneous structures are, most likely, poorly conducting metals displaying ohmic behavior. In contrast, the bilobed structures may include a Schottky barrier and, hence, may display rectifying diode behavior. If so, the transport properties of the two structures are expected to be markedly different and this difference may be technologically useful as a phase-change material.[9]

The proposed transformation cycle is sketched schematically in Fig. 5.[4,10] At high temperatures, above T_m, the nanostructures are liquid. Rapid cooling (such as that during PLM experiments) first supercools the liquid and then leads to the formation of a single metastable phase homogeneous in composition at a temperature T_g. In the case of pure Ge and, most likely, GeSn, this structure is amorphous. In the case of GeAu, there is evidence for the formation of hexagonal close-packed β-phase. Reheating this structure to above T_g (but below T_m) during RTA leads to subsequent solidification into a crystalline phase at temperature T_{crys}. At this point, it is not clear if the metastable phase formed during PLM first melts and then recrystallizes or if this phase transforms directly into the crystalline phase.

The parameters T_g, T_{crys}, and T_m are likely to depend on a number of experimentally controllable factors, and it is worth exploring this dependence.

To date, we have considered the composition dependence T_{crys} within GeSn alloys. More specifically, we grew a number of nanostructures using IBS with differing ratios of Sn:Ge ranging from 0 to 1. The samples were processed using PLM (again a 30-ns

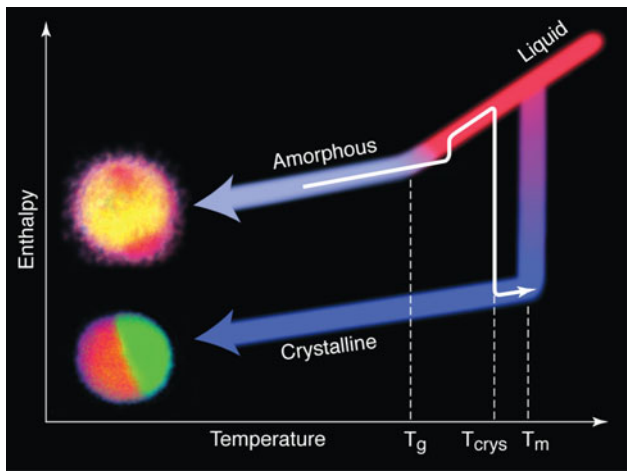

Fig. 5. A schematic of the phase transformations studied within BEANs. Starting from the liquid state, rapid cooling below T_g leads to nearly compositionally homogeneous structures. Subsequent reheating to above T_g leads to remelting and subsequent formation of the bilobed state at temperature T_{crys} (white arrow). Further heating then leads to melting; alternatively, cooling retains the bilobed structure (from Ref. 4) (Color figure online).

pulse of 248-nm light with an energy density of 0.3 J/cm^2), and then subjected to RTA for 10 s at varying temperatures. Since the PLM leads to amorphization of pure Ge nanocrystals, we gauge the crystallinity of the samples subjected to RTA using Raman scattering. The Raman response for amorphous Ge is well known, as is the Raman signal for Ge nanocrystals. Amorphous Ge gives a broad Raman response, with intensity beginning at roughly 300 cm^{-1}, and spreading to lower wave numbers.[2] In contrast, the peak arising from Ge nanocrystals is relatively sharp and slightly asymmetric due to the finite size of the nanocrystals. One can, therefore, use the width of the Raman peak as a gauge of the crystallinity of the sample. Using this approach, we note that recrystallization temperatures for GeSn nanostructures can be varied between approximately 150°C and 550°C simply by altering the composition.[4] The recrystallization kinetics are thus tunable over a broad range. A similar study performed for the GeAu system shows that reequilibration in that system can take place at temperatures as low as 80°C.

CONCLUSIONS

As mentioned, nanostructures are known to display a host of remarkable properties. Embedding these same nanostructures within a matrix increases the range of behaviors accessible to experiment (and technology). For example, in the past we have shown that Ge nanocrystals embedded within SiO_2 display a very large melting/solidification hysteresis nearly centered on the bulk melting point.[11] This behavior is simply not expected within a bulk material, and it emerges because of the properties of the Ge/SiO_2 interfaces and the fact that at the nanoscale, interfaces contribute substantially to the free energies governing thermodynamic stability and the kinetics of phase transformations.

In the case of BEANs embedded within silica, a still broader range of behavior is experimentally accessible. Not only are the melting/solidification kinetics altered from those expected in bulk alloys, but also the range of accessible states is expanded: The extreme cooling rates accessible within PLM experiments of nanostructures stabilizes compositionally homogeneous states that would otherwise be inaccessible experimentally. Thus, there is the possibility that one can stabilize and characterize new structures.

In the current work, we have discussed two types of BEANs in which this principle has been demonstrated explicitly: GeSn and GeAu nanostructures. Using PLM, both can be stabilized in structures that are nearly compositionally homogeneous. Furthermore, both can be transformed toward their equilibrium, bilobed/bicrystalline states using RTA. We have proven that the transformation temperature can be controlled using composition and have argued that the electronic properties of the two phases are substantially different.

These differences in properties might be exploited to create a memory device, for example. Discerning the difference between ohmic and rectifying behavior should be straightforward, provided that electrical contact can be made to the BEANs. Such contact would be facilitated by fabricating BEANs within a wire geometry, for example.[12]

The two different structures are likely to display differing thermodynamic response as well. For example, one expects the temperature dependence of the heat capacity for the two structures to differ. Such differences might be exploited to tune the thermal properties of a matrix/BEAN composite to obtain an optimal thermal response. Such materials might find applications within the broad area of thermal storage and transport.

Moreover, one expects that with further knowledge of transformation kinetics, other states might also become accessible to BEANs. For example, we have only considered the limits of equilibrium and very rapid solidification. For the equilibrium case, we imagine that only one Ge nuclei forms at the SiO_2/liquid alloy boundary, and that this nuclei gives rise to a single Ge lobe during the remainder of the crystallization. This does not have to be the case. In the extreme case, one might form a large enough number of nuclei on the surface of BEAN to form a kinetically stabilized core/shell structure.

ACKNOWLEDGEMENTS

This work was supported by the Director, Office of Science, Office of Basic Energy Sciences, Division of Materials Sciences and Engineering, of the U.S. Department of Energy under contract no. DE-AC02-05CH11231.

REFERENCES

1. X.G. Peng, J. Wickham, and A.P. Alivisatos, *J. Am. Chem. Soc.* 120, 5343 (1998).
2. I.D. Sharp, Q. Xu, C.Y. Liao, D.O. Yi, J.W. Beeman, Z. Liliental-Weber, K.M. Yu, D.N. Zakharov, J.W. Ager, D.C. Chrzan, and E.E. Stable Haller, *J. Appl. Phys.* 97 (2005).
3. C.W. Yuan, S.J. Shin, C.Y. Liao, J. Guzman, P.R. Stone, M. Watanabe, J.W. Ager, E.E. Haller, and D.C. Chrzan, *Appl. Phys. Lett.* 93, 193114 (2008).
4. S.J. Shin, J. Guzman, C.W. Yuan, C.Y. Liao, C.N. Boswell-Koller, P.R. Stone, O.D. Dubon, A.M. Minor, M. Watanabe, J.W. Beeman, K.M. Yu, J.W. Ager, D.C. Chrzan, and E.E. Haller, *Nano Lett.* 10, 2794 (2010).
5. J. Guzman, C.N. Boswell-Koller, J.W. Beeman, K.C. Bustillo, T. Conry, O.D. Dubon, W.L. Hansen, A.X. Levander, C.Y. Liao, R.R. Lieten, C.A. Sawyer, M.P. Sherburne, S.J. Shin, P.R. Stone, M. Watanabe, K.M. Yu, J.W. Ager, D.C. Chrzan, and E.E. Haller, *Appl. Phys. Lett.* 98, 193101 (2011).
6. J.H. Wernick, *J. Chem. Phys.* 25, 47 (1956).
7. D.P. Brunco, J.A. Kittl, C.E. Otis, P.M. Goodwin, M.O. Thompson, and M.J. Aziz, *Rev. Scientif. Instrum.* 64, 2615 (1993).
8. C.A. Sawyer, J. Guzman, C.N. Boswell-Koller, M.P. Sherburne, J.P. Mastandrea, K.C. Bustillo, J.W. Ager, E.E. Haller, and D.C. Chrzan, *J. Appl. Phys.* 110, 094307 (2011).
9. M. Wuttig and N. Yamada, *Nat. Mater.* 6, 824 (2007).

10. S.O. Kasap and P. Capper, *Handbook of Electronic and Photonic Materials* (New York: Springer, 2006), p. 1406.
11. Q. Xu, I.D. Sharp, C.W. Yuan, D.O. Yi, C.Y. Liao, A.M. Glaeser, A.M. Minor, J.W. Beeman, M.C. Ridgway, P. Kluth, J.W. Ager, D.C. Chrzan, and E.E. Haller, *Phys. Rev. Lett.* 97, 155701 (2006).
12. Y.L. Chueh, C.N. Boswell, C.W. Yuan, S.J. Shin, K. Takei, J.C. Ho, H. Ko, Z.Y. Fan, E.E. Haller, D.C. Chrzan, and A. Javey, *Nano Lett.* 10, 393 (2010).
13. L. Balde, B. Legendre, and A. Balkhi, *J. Alloys Comd.* 216, 285 (1995).